A composite approach to Al2O3 based plasma-sprayed coatings

Olivier Amsellem, François Borit, Vincent Guipont, Michel Jeandin, F. Pauchet

A Composite Approach to Al_2O_3-based Plasma-Sprayed Coatings

O. Amsellem, F. Borit, V. Guipont and M. Jeandin
Ecole des Mines de Paris, Materials Research Center PM Fourt/ UMR CNRS 7633 – C2P, Center for Plasma Processing, BP 87, 91003 Evry Cedex , France.
Email address: michel.jeandin@ensmp.fr

F. Pauchet
Schlumberger, Riboud Product Center, 1, rue Henri Becquerel, 92140 Clamart, France.

Abstract

Thermally-sprayed ceramic coatings such as plasma-sprayed alumina show a composite microstructure actually due to the presence of defects such as pores, inter-lamellar and intra-lamellar cracks. These 2nd phase-typed features influence the mechanical behavior and electrical insulation of the coating dramatically. In this study, a composite approach to the microstructure of plasma-sprayed alumina was developed for the optimising of component properties such as electrical gaps used in the oil industry. This approach consisted of a Finite Element Analysis (FEA) of thermo-mechanical and electrical properties from simulated microstructures. Series of composite microstructures were tested, i.e that of air plasma-sprayed (APS) alumina basically plus those obtained by addition of glass or resin using co-spraying and impregnation respectively. Various degrees of porosity and cracks could be obtained from different spraying conditions and by subsequent laser surface remelting. Every composite microstructure was studied using quantitative image analysis of series of SEM cross-sections. Electrochemical Impedance Spectroscopy (EIS) in NaCl solution was also performed to characterize the level of connected pores and the resulting electrical insulating properties. From experiments, a Finite Element Model (FEM) based on the actual microstructure was developed. The latter was simulated with involving of all significant features, such as phase distribution, porosity and defects. This simulation was developed to optimize the composite microstructure to meet industrial applications.

Introduction

Thermal spraying is a prominent process for depositing low-cost high-performance dielectric coatings such as those made of pure alumina (Al_2O_3). Al_2O_3 is used extensively for its electrical insulating properties because of its high dielectric strength [1]. Thermal spraying is a deposition process in which molten particles impact at a high velocity, spread and solidify onto a substrate to form thin lamellae. Consequently, thermally-sprayed alumina coatings show a composite microstructure due to the presence of defects such as pores, inter-lamellar and intra-lamellar cracks. These defect origins are multiple. First, build-up defects and gas entrapped generate specific inter-lamellar cracks and pores. Second, intra-lamellar microscopic cracks may be achieved due to rapid solidification after spreading, especially for ceramic materials. The combination of these features generates an interconnected network of pores and cracks. These 2nd phase-typed features influence the mechanical behavior and electrical insulation of the coating dramatically [2,3]. In order to know their influence, authors described physical properties as a function of coatings microstructure for the plasma processing [4,5,6]. This work was carried out to good deepen into this microstructure-properties approach through the development of coating. This approach has been used in the conventional composite material area and in powder metallurgy. However, for plasma-sprayed coating only few attempts can be noticed because of the intricacy of the involved microstructure [7,8]. This work was based on the study of composite microstructures obtained by air plasma spraying (APS) including those obtained by addition of glass or resin using co-spraying and impregnation respectively. Quantitative Image Analysis (QIA) was applied to coatings obtained using different spraying procedures and subsequent laser surface remelting. Electrochemical Impedance Spectroscopy (EIS) was performed to determine the physical and electrical characteristics of the ElectroChemical Interface (ECI). This technique was extensively employed to study corrosion phenomena [9,10]. EIS was used to correlate the microstructure with coating properties only in the past recent years [11,12,13,14]. The objective was to achieve the EIS spectra of thick (400 µm) and highly-dense (porosity <6%) alumina composite coatings. Then, methods can be envisaged to investigate into the thermo-mechanical behavior of the coating i.e., first a model based on a statistical study of composite phases [8,15] and, second, a model based on the actual coating microstructure [9,16]. The first model disregards some features of the microstructure. This contribution shows a Finite Element Model (FEM) based on the actual microstructure which allows characterization of all the composite microstructure features and that of thermo-mechanical properties of coating.

Materials and Processes

Thermal spraying

APS alumina composites were sprayed onto grit-blasted stainless steel plates (AISI 304L, 25×30×2 mm^3, Ra≈ 4µm) with a F4-VB Sulzer Metco torch (Table 1). The scanning step and velocity of the torch were equal to 5mm.$pass^{-1}$ and 200mm.s^{-1} respectively. Two air-cooling jets were added close to the torch in order to lower the coating temperature, limit thermal stresses and consequently avoid adhesion problems. Two commercial powders were used, i.e. 105 SFP alumina from Sulzer Metco/Wohlen for alumina and P3000 glass from Potters-Ballotini/Barnsley.

Table 1: Plasma spraying parameters

Sample	A	B	C	D	E	F	G	
Powder	105 SFP						105 SFP	P3000
Mode	APS						APS co-spraying	
Intensity (A)	530	530	530	530	530	600	530	
Spraying distance (mm)	130	110	130	130	90	130	130	
Ar gas (l.min^{-1})	41	41	41	30	41	41	41	
H_2 gas (l.min^{-1})	14	14	14	8	14	14	14	
Powder (g.min^{-1})	20	20	20	20	20	20	20	2.5
Injector diameter (mm)	1.8	1.8	1.5	1.8	1.8	1.8	1.8	1.8
Injection gas (l.min^{-1})	3.4	3.4	3.4	3.4	3.4	3.4	3.4	3.4

Post-treatment

Impregnation [17,18] and laser surface melting of thermal spray coatings were used to seal and/or modify the composite microstructure. The selected sealants were commercial polymers: epoxy and polyurethane resin (Metcoseal URS and ERS). Prior to post-treatment, the as-sprayed samples were cleansed in an ultrasonic bath of ethanol. Laser glazing of plasma-sprayed alumina composite was carried out using a KrF excimer laser radiation (λ=248 nm), operating at 60 Hz. The laser fluence and the number of pulses ranged from 2 to 8 J.cm^{-1} and from 80 to 500 pulses respectively. The laser beam was shaped using a rectangular mask and focused on the sample surface to achieve laser-treated areas of about 3.5×1.2mm^2. The velocity of the laser beam was equal to 3cm.s^{-1} respectively. All experiments were carried out in air.

Quantitative Image Analysis

Every Al_2O_3 composite microstructure was studied using quantitative image analysis of series of SEM images (LEO1450VP). To meet criteria for statistics, 15 SEM digitalized images (764×1024 $pixels^2$) at a magnification of ×1500 were recorded per coating. Back-scattering electrons were used to enhance the image contrast of voids and defects. Cross-sectioned specimens were metallized (Au-Pd film = 3nm) prior to SEM acquisition. Quantitative image analysis (QIA) consisted in multi-stage processing using "MATLAB" software [5]. X-ray diffractometer and Electron Probe MicroAnalyzer (EPMA) were then used to identify the phases in the composite coating.

Electrochemical Impedance Spectroscopy (EIS)

EIS is an electrochemical method in which an AC signal $E(t)=E_0\sin(\omega t)$ is applied to an electrode in an aqueous solution. Current as a function of time, i.e. $I(t)=I_0\sin(\omega t+\phi)$ is measured to give the impedance at different frequencies, which results in the impedance spectrum $Z(\omega)=E(t)/I(t)$. Electrochemical characteristics of the cell are determined from modelling and interpretation of EIS spectra. EIS measurement was performed at room temperature with two different facilities to obtain $Z(\omega)$ in a large range of frequencies. A Solartron 1250 Frequency Response Analyzer (FRA) was connected to Solartron 1287 Electrochemical Interface for impedance between f=0.005Hz and 65kHz. A Hewlett-Packard 4192 Electrochemical Interface was used between f=5Hz and 13MHz. Experiments were carried out in a 30g.l^{-1} NaCl aqueous solution in the 2-electrode mode. The working electrode was the coating and the counter electrode a platinum grid. The electrochemical test cell was a specifically-designed cell which allowed the control of the area coating-electrolyte interface and the electrode distance. The samples were immersed 10min in the solution before measuring to fill the open porosity. Then, a sinusoidal variation of 0.1V was applied and the impedance spectra were achieved after given time intervals.

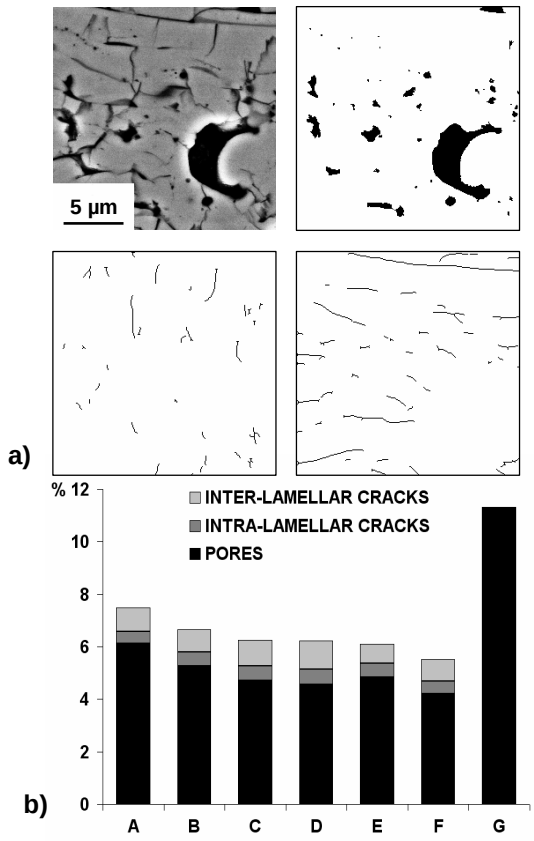

Fig. 2: Microstructure analysis a) Q.I.A. processing stages b) Composite porosity and cracks.

Finite Element Model

Elastic properties were studied for all types of sprayed Al_2O_3 composites. A Finite Element Model (FEM) based on the actual microstructure was developed in Zebulon®. With this FEM code, mapping of digitalized image was obtained onto a finite element mesh.

Results and discussion

Composite microstructures

It was shown that the microstructure of thermally-sprayed coating can be described as an Al_2O_3-based composite with different features related to the matrix and defects (nature, content, orientation). The series of SEM digital images allowed to measure the porosity and crack contents to achieve the quantitative study of the microstructure defects (Figure 2b). Further "crack" images (Figure 2a) were processed by skeletizing, which limited crack defect thickness to only 1 pixel and deleted triple points and their first neighbouring point). From the skeletized "crack" image, both inter lamellar cracks (main orientation <45°) and intra-lamellar cracks (main line orientation >45°) could be discriminated easily using an automatic orientation criterion. X-ray and Electron-Probe Micro-Analysis (EPMA) showed that the matrix coating mainly consisted in cubic γ-Al2O3 with a small amount of body-center α-Al2O3 in unmelted particles. Na impurity which comes from the starting powder was detected in a few particles. Co-spraying process led to a glass-alumina matrix with 20% of glass (Figure 4). The EPMA showed a good building-up of the lamellae of alumina and glass. It can be noticed that the glass splats are much thicker than those of alumina and there were no cracks in the glass phase. On the other hand, the use of sealing or laser post-treatment led to another type of complex composite structure. In the sealing process, vacuum was applied to the sample with resin before sealing to remove the residual air from the pores and improve the impregnation depth. EPMA carbon X-ray map showed that porosity had been impregnated till a depth of 600 µm. As for laser post-treatment, the effects of laser parameter on the surface of alumina coating were studied (Figure 3). Crater formation (figure 3b) and microstructure modification on 10µm depth (figure 3c, 3d) were observed from the free surface of the coating. Because of a small wavelength combined to a short pulse duration and a high power density of the excimer laser, only a very thin layer near the material surface could be treated without cracks.

Electrochemical Testing

There are two conventional diagrams for data and results, i.e. the Bode (|Z| and ϕ vs ω) and Nyquist (Z_{Im} along the Y-axis and Z_{Re} along the X-axis vs ω) plots respectively. Figure 5 shows the typical response of alumina composite coating using both diagrams (Zview®). Three time constants were observed in the frequency range from 0.05 Hz to 13 MHz. Based on the typical spectra shown in Figure 5 and on the morphological structure of the cell system, an EIS equivalent circuit (EC) was proposed. This circuit which is an assembly of circuit elements (resistors, capacitors, inductors, and various forms of impedances) gives, at all frequencies, the same response as the system of the study. Information on the electrochemical cell could therefore be extracted through an appropriate interpretation of the EC variables. Theses variables represent the physical and electrical characteristics of the different

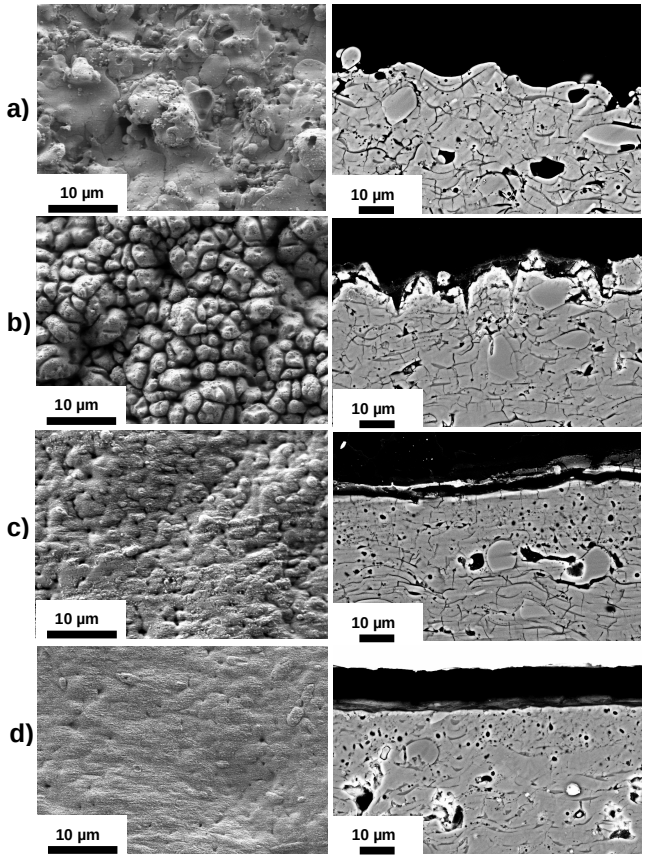

Fig. 3: Composite microstructures a)As-sprayed alumina surface and cross section b) 2J.cm^2 - 500 pulses :Crater formation and crater cross-section c) 6.2J.cm^2 - 250 pulses: surface and cross section d) 8J.cm^2 - 250 pulses: surface and cross section.

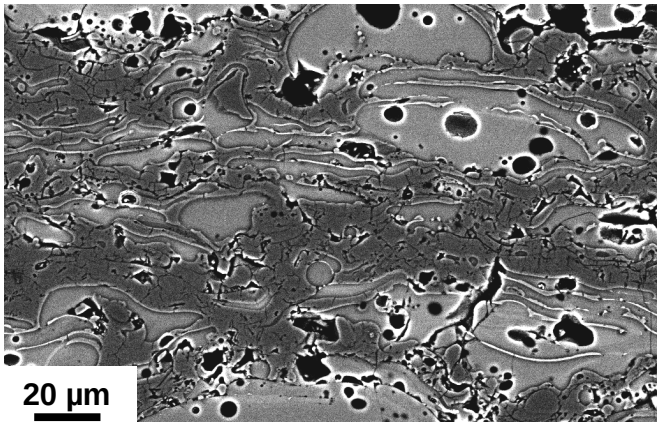

Fig. 4: Alumina-glass composite

electrochemical interfaces in the system. Coating steel exposed to an aqueous solution has been investigated by several authors [11,12,14,19]. An EC as that shown in Figure 6a is generally proposed to describe the different electrochemical interfaces where the substrate is exposed to the electrolyte through permeable defects. The electrolyte is a resistor, represented by R_e, in series with the first electrolyte-ceramic interface which consists of a capacitor C_c and a resistor R_c. C_p and R_p simulates the electrochemical reaction in the permeable

defects. Then, C_s and R_s result in the interface between the ceramic coating and the substrate. The capacitances were replaced by a Constant-Phase-Element (CPE) because of the heterogeneity in the cell system [20]. These measures were duplicated 100 times for good statistics and to take account the corrosion which occurred at the substrate interface during the experiment (Figure 6b-c). Electrochemical results can be correlated with the alumina composite microstructure (2.1). The resistance of the electrolyte in the porosity (R_p) decreased when coating porosity increased (Ref.: A, D, F). EIS in aqueous solution was shown to be powerful to correlate microstructure defects with the electrical properties of composites.

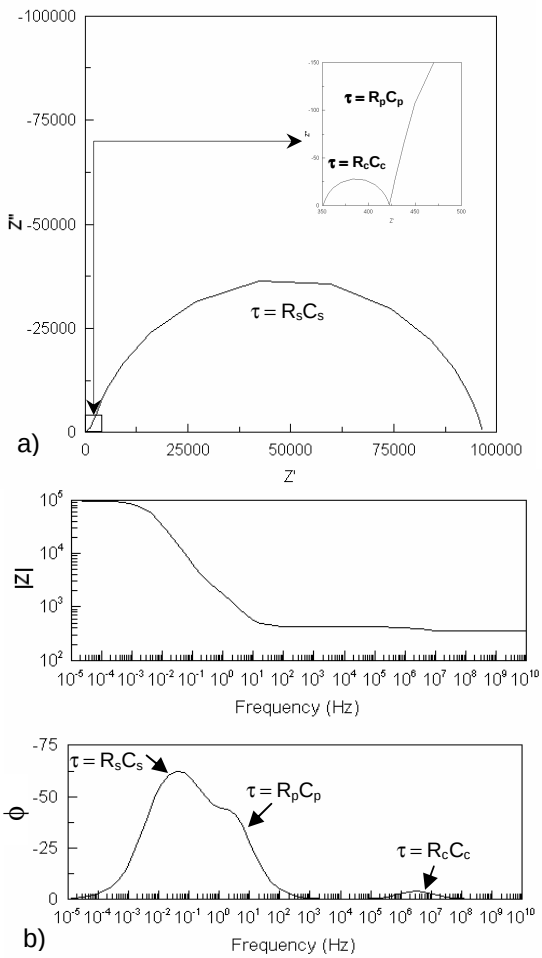

Fig. 5: Electrochemical response of alumina composite a)Nyquist and b)Bode diagrams

FEM

The microstructure of the composite considered with all the significant features like phase distributions, porosity and defects and related relevant material properties ($E_{ALUMINA}$= 224GPa). The finite element mesh was generated and refined until it met sufficient microstructure details (Figure 7). In this work, cross-section composites from QIA (see Part 2.2.1) were used to generate microstructure-based finite element meshes. FEM was developed to find a compromise between meshing accuracy and computational time. All simulations were performed in the plane strain hypothesis. The optimal alumina composite representative area (a square image of 71µm in) was determined with successive tests at different image scales. Numerical models succeed in representing anisotropy through the moduli along spray (Es=53GPa) and transverse (Et=96GPa) direction.

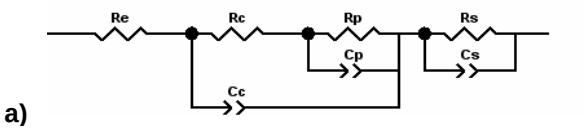

a)

b)

	Re + Rc (Ω)	Rp (Ω)	Cp (µF)	Cs (µF)
Ref. A	365 ± 18	1044 ± 52	0.57 ± 0.028	0.85 ± 0.043
Ref. D	367 ± 18	1538 ± 77	0.39 ± 0.019	0.67 ± 0.033
Ref. F	376 ± 19	1687 ± 84	0.26 ± 0.013	0.45 ± 0.023

c)

Fig. 6: EIS experiments a)Equivalent circuit b)Table result c)R_p measurement, see Table1 for Ref. details.

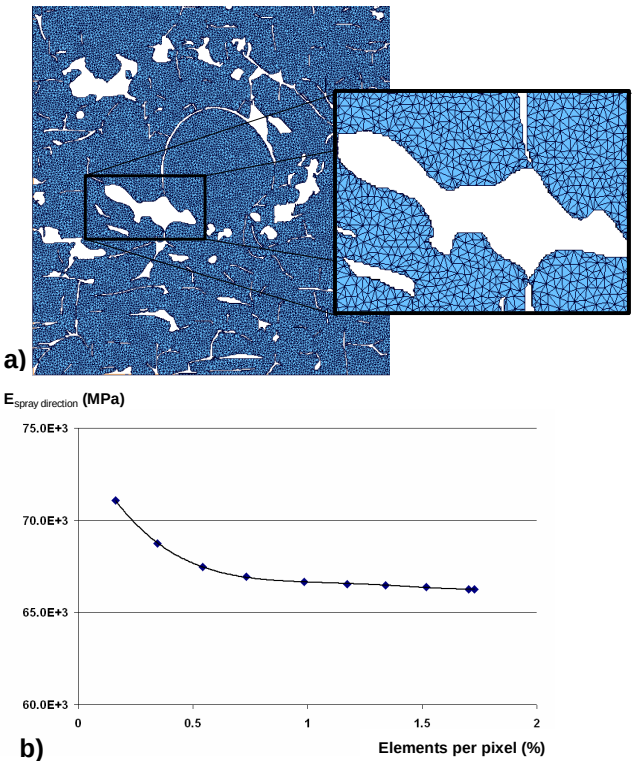

Fig. 7: FEM experiments, a)Finite element mesh b)Moduli along spray direction function of element density.

Conclusions

Different types of composites were obtained using several processes. APS single spraying and co-spraying led to several alumina-defect composites and alumina-glass-defect composites respectively. In post-processing, the pores were filled with resin and excimer laser was used to modify the surface of as-sprayed alumina composite. Quantitative Image Analysis (QIA) was developed to determine the degree of porosity. EIS allowed the correlating of the microstructure with physical coating properties. It described the coating network architecture especially. Then, a FEM model based on actual microstructure was implemented in order to evaluate the effective elastic moduli and thermal conductivity along the spray and transverse directions of the various alumina composites. All results ascertained the so-called "composite approach" to plasma sprayed materials to establish relationship between microstructure and properties.

Acknowledgments

The authors are indebted to Dr P. Delaporte from LP3 UMR 6182 CNRS-France for the excimer treatment.

References

[1] Gadow, R. *et al*, "Combined metallurgical and ceramic coating in the development of tubular ozone generators", *Proc 15th International Thermal Spray Conf*, Nice,France, May. 1998, pp. 1083-1089.

[2] Pawlowski L. *et al*, "The relationship between structure and dielectric properties in plasma sprayed alumina coating", *Surface & Coatings Technology*, Vol. 35, (1988), pp. 285-298.

[3] Beauvais S. *et al*, "Influence of defect orientation on electrical insulating properties of plasma-sprayed alumina coatings", *Journal of electroceramics*, Vol. 15, (2005), pp. 65-74.

[4] Li C. J. *et al*, "Relationships between the Microstructure and properties of thermally sprayed deposits, *Journal of Thermal Spray Technology"*, Vol. 11, (2002), pp. 365-374.

[5] Beauvais S. *et al*, "Process-Microstructure-Property relationships in controlled atmosphere plasma spraying (CAPS) of ceramics", *Surface and Coating Technology*, Vol. 183, (2004), pp. 204-211.

[6] Sarikaya O. *et al*, "Effect of some parameters on microstructure and hardness of alumina coatings prepared by air plasma spraying", *Surface & Coatings Technology*, Vol. 190, (2005), pp. 388-393.

[7] Bolelli G. *et al*, "Glass-alumina composite coatings by plasma spraying. Part I: Microstructural and mechanical characterization", *Surface & coating Technology*, Vol. 201, (2006), pp. 458-473.

[8] Wang Z. *et al*, "Effects of pores and interfaces on effective properties of plasma sprayed zirconia coatings", *Acta Materialia*, Vol. 51, (2003), pp.5319-5334.

[9] Creus J. *et al*, "Porosity evaluation of protective coatings onto steel, through electrochemical techniques", *Surface & Coatings Technology*, Vol. 130, (2000), pp. 224-232.

[10] Antou G. *et al*, "Characterizations of the pore-crack network architecture of thermal-sprayed coatings", *Materials Characterization*, Vol. 53, (2004), pp.361-372.

[11] Saenger R. *et al*, "Electrochemical characterization of plasma sprayed WC-Co coatings by impedance techniques", *Surface & Coatings Technology*, Vol. 194, (2004), pp. 335-343.

[12] Zhang J. *et al*, "Evaluation of thickness, porosity and pore shape of plasma sprayed TBC by electrochemical impedance spectroscopy", *Surface & Coatings Technology*, Vol. 190, (2005), pp. 98-109.

[13] Byeon J.W. *et al*, "Non-destructive evaluation of degradation in multi-layered thermal barrier coatings by electrochemical impedance spectroscopy", *Materials Science & Engineering A*, Vol. 407, (2005), pp.213-225.

[14] Liu C *et al*., "An electrochemical impedance spectroscopy study of the corrosion behaviour of PVD coated steels in 0,5 N NaCl aqueous solution: Part I. Establishment of equivalent circuits for EIS data modelling", *Corrosion Science*, Vol. 45, (2003), pp.1243-1256.

[15] Sevostianov I. *et al*, "Plasma-sprayed ceramic coatings: anisotropic elastic and conductive properties in relation to the microstructure; cross-property correlations", *Materials & Science Engineering A*, Vol. 297, (2001), pp. 235-243.

[16] Bolelli G. *et al*, "Glass-alumina composite coatings by plasma spraying. Part II: Microstructure-based modelling of mechanical properties", *Surface & coating Technology*, Vol. 201, (2006), pp. 474-486.

[17] Wielage B. *et al*, "Improving the Resistivity of Thermal Sprayed Coatings", *Surface Modification Technologies*, Vol. XI, (1998), pp.328-335.

[18] Knuuttila J. *et al*, "Sealing of thermal spray coatings by impregnation", *Journal of thermal spray technology*, Vol. 8(2), (1998), pp. 1999-249.

[19] Cottis R., *Electrochemical Impedance and Noise*, Nace International, (1999).

[20] Jiang S.P *et al*, "Electrochemical Techniques in Studies of Solid ionic Conductors", *Key Engineering Materials*, Vol. 125-126, (1997), pp. 81-132.